

1 **Comprehensive analysis of miRNA and protein profiles within exosomes derived**  
2 **from canine lymphoid tumour cell lines**

3

4 Hajime Asada<sup>1¶</sup>, Hirotaka Tomiyasu<sup>1¶\*</sup>, Takao Uchikai<sup>2</sup>, Genki Ishihara<sup>2</sup>, Yuko  
5 Goto-Koshino<sup>1</sup>, Koichi Ohno<sup>1</sup>, and Hajime Tsujimoto<sup>1</sup>

6

7 *<sup>1</sup>Department of Veterinary Internal Medicine, Graduate School of Agricultural and Life*  
8 *Sciences, The University of Tokyo, Bunkyo-ku, Tokyo, Japan*

9 *<sup>2</sup>Anicom Specialty Medical Institute Inc., Shinjuku-ku, Tokyo, Japan*

10

11 ¶These authors equally contributed to this study.

12

13 \*Corresponding author

14 E-mail address: [atomi@mail.ecc.u-tokyo.ac.jp](mailto:atomi@mail.ecc.u-tokyo.ac.jp) (HT)

15

## 16 **Abstract**

17       Exosomes are small extracellular vesicles released from almost all cell types,  
18 which play roles in cell-cell communication. Recent studies have suggested that  
19 microenvironmental crosstalk mediated by exosomes is an important factor in the  
20 escape of tumour cells from the anti-tumour immune system in human haematopoietic  
21 malignancies. Here, we conducted comprehensive analysis of the miRNA and protein  
22 profiles within the exosomes released from four canine lymphoid tumour cell lines as a  
23 model of human lymphoid tumours. The results showed that the miRNAs and proteins  
24 abundantly contained in exosomes were similar among the four cell lines. However, the  
25 profiles of miRNA within exosomes differed among the cell lines and reflected the  
26 expression pattern of miRNAs of the parent cells. In the comparison of the amounts of  
27 miRNAs and proteins among the cell lines, those of three miRNAs (miR-151,  
28 miR-8908a-3p, and miR-486) and CD82 protein differed between exosomes derived  
29 from vincristine-sensitive and resistant cell lines. Further investigations are needed to  
30 elucidate the biological functions of the exosomal contents in the microenvironmental  
31 crosstalk of lymphoid tumours.

32

## 33 **Introduction**

34 Exosomes are small extracellular vesicles released from almost all cell types,  
35 including immune cells and tumour cells [1], as the intracellular endosome component.  
36 Although exosomes were initially considered cellular waste, they have been shown to  
37 contain various molecules from the original cells, including proteins, functional mRNAs  
38 and miRNAs, and deliver these biological messages into the recipient cells [1,2]. To  
39 date, it has also been reported that tumour cells release a number of exosomes and they  
40 stimulate tumour cell growth and modify the immune cell response to promote tumour  
41 progression and metastasis in several human tumors, including colorectal cancer [3],  
42 breast cancer [4], melanoma [5], and pancreatic cancer [6]. Thus, the interaction  
43 between tumour cell-derived exosomes and recipient cells in the microenvironment of  
44 solid tumours is considered an important factor in tumour progression, metastasis, cell  
45 survival, and escape from the anti-tumour immune system.

46 Exosomes have also been suggested to play important roles in the  
47 microenvironmental crosstalk of human haematopoietic tumours, including leukaemia  
48 and lymphoma [7,8]. It has been reported that exosomes derived from acute/chronic  
49 myeloid leukaemia and lymphoma cells inactivate natural killer cells and suppress the  
50 anti-tumour immune response [7-9]. In addition, exosomes have been reported to be

51 associated with drug resistance in these tumours [7]. For instance, it was reported that  
52 exosomes derived from imatinib-resistant chronic leukaemia cells could confer  
53 imatinib-resistance traits into sensitive cells by delivering miR-365 [10]. It was also  
54 reported that exosomes derived from bone marrow stromal cells decreased the  
55 sensitivity of acute lymphoblastic leukaemia cells to etoposide [11]. Based on this  
56 background information, it has been considered that studies on the molecules contained  
57 in exosomes released from haematopoietic tumour cells could provide insight into the  
58 pathophysiology of these tumours. Although the miRNA profile within exosomes was  
59 reported in Gamma-Herpesvirus-infected lymphoma cell lines [12] and lymphocytic  
60 leukaemia cells [13], no study has yet comprehensively analysed the miRNA and  
61 protein profiles of exosomes derived from haematopoietic malignancies.

62 Lymphoma is a haematopoietic malignancy originating from lymphoid cells, and  
63 it is categorised into more than 80 distinct subtypes [14]. Among them, Non-Hodgkin  
64 lymphoma (NHL) is the most common type of lymphoma in humans and dogs [15]. It  
65 has been reported that canine lymphoma shares many characteristics of human NHL,  
66 including clinical presentation, immunophenotypic composition, chemotherapeutic  
67 protocols, and response to treatment [15,16]. Therefore, canine lymphoma has been  
68 advocated as an ideal model for studying human NHL [15,16].

69 The aim of this study was to comprehensively analyse the miRNA and protein  
70 profiles within the exosomes released from canine lymphoid tumour cells.

## 71 **Results**

### 72 **Exosome isolation and preparation of total RNA of exosomes** 73 **and parent cells**

74 The size distributions of exosomes isolated from four canine lymphoid tumour  
75 cell lines, CLBL-1, GL-1, UL-1, and Ema, are shown in S1 Fig. The average size was  
76 between approximately 100–150 nm in each cell line. The RNA integrity numbers  
77 (RINs) and size distributions of total RNA samples taken from exosomes and parent  
78 cells are shown in S2 Fig. Although there were common peaks corresponding to  
79 ribosomal RNAs in exosomal RNA of the four cell lines, the distributions of RNA sizes  
80 were clearly different between exosomes and parent cells.

### 81 **Exosomal miRNA profiles**

82 At first, the miRNA profiles of exosomes and parent cells were investigated via  
83 small RNA sequencing analysis. A minimum of 20 million raw reads were generated  
84 for each sample (see S1 Table). The number of reads mapped to miRNA and the  
85 mapping rate to miRNA was comparatively lower in Ema than the other three cell lines.  
86 Therefore, data for Ema were omitted in the statistical comparison of the quantities of

87 miRNAs among cell lines using small RNA sequencing data.

88 Then, hierarchical clustering using the amounts of miRNA in CLBL-1, GL-1, and  
89 UL-1 was conducted. This analysis yielded three clusters composed of exosomes and  
90 parent cells of each cell line (Fig 1a). In addition, in the PCA plots, exosomes and cells  
91 clustered similarly for each cell line (Fig 1b). The results of these analyses were similar  
92 when the data from Ema were included (see S3 Fig).

93

94 **Fig 1. Hierarchical clustering (a) and PCA plots (b) for miRNA profiles of**  
95 **exosomes and parent cells of CLBL-1, GL-1, and UL-1.** Exosomes and parent cells  
96 clustered similarly for each cell line and the profiles were different among cell lines.  
97 Orange dots (exosomes) and red dots (parent cells) correspond to CLBL-1, violet dots  
98 (exosomes) and blue dots (parent cells) to GL-1, and grey dots (exosomes) and black  
99 dots (parent cells) to UL-1.

100

101 The top ten miRNAs contained in exosomes and parent cells are listed in Table 1.  
102 Among these miRNAs, five miRNAs (let-7f, let-7g, miR-7, miR-30d, and miR-92a)  
103 were commonly contained in exosomes and cells of the four cell lines.

104

**Table 1. The top 10 miRNAs abundantly contained in the exosomes and parent cells in this study.**

CLBL-1		GL-1		UL-1		Ema	
Exosome	Parent cell	Exosome	Parent cell	Exosome	Parent cell	Exosome	Parent cell
miR-148a	miR-148a	miR-148a	miR-148a	miR-7	miR-7	miR-7	let-7g
miR-7	let-7g	let-7f	let-7g	miR-378	miR-99a	let-7g	miR-7
let-7g	miR-363	let-7g	miR-10a	miR-99a	miR-378	let-7f	miR-363
let-7f	miR-7	miR-30d	let-7f	miR-30d	miR-30d	miR-30d	let-7f
miR-146a	miR-99a	miR-10a	miR-30d	let-7g	let-7g	miR-363	miR-30d
miR-30d	miR-30d	miR-378	miR-378	let-7f	miR-10a	miR-21	miR-21
miR-99a	miR-128	miR-7	miR-7	miR-363	miR-363	miR-148a	miR-128
miR-20a	miR-92a	let-7a	miR-128	miR-10a	miR-128	miR-26a	miR-26a
miR-378	let-7f	miR-103	miR-21	miR-92a	let-7f	miR-155	miR-92a
miR-92a	miR-146a	miR-92a	let-7a	miR-103	miR-25	miR-92a	miR-155

106 In the comparison of the amounts of miRNAs between cells and exosomes, the  
107 amounts of 39, 20, and 24 miRNAs were significantly different in CLBL-1, UL-1, and  
108 Ema, respectively ( $q < 0.01$ ) (Fig 2). Among these miRNAs, the amount of miR-350  
109 was significantly higher in exosomes than parent cells in all the three cell lines, and  
110 those of miR-22, miR-671, and miR-8865 were significantly lower in exosomes than  
111 parent cells in these cell lines (see S4 Fig). On the other hand, no miRNA displayed a  
112 significant difference in amount between exosomes and cells in GL-1.

113

114 **Fig 2. Heat maps showing the miRNAs whose amounts were significantly different**  
115 **between exosomes and parent cells of CLBL-1 (a), UL-1 (b), and Ema (c).** The  
116 amounts of 39, 20, and 24 miRNAs were significantly different in CLBL-1, UL-1, and  
117 Ema, respectively ( $q < 0.01$ ).

118

119 The difference in the amount of miR-350 between exosomes and parent cells was  
120 confirmed by RT-qPCR (Fig 3). However, the amounts of miR-22, miR-671, and  
121 miR-8865 were not significantly different between exosomes and parent cells according  
122 to RT-qPCR. Following quantitative analysis, prediction of target genes was conducted  
123 for miR-350 using miRbase, and the top 10 target genes of the miRNA were extracted



124 (see S2 Table). These target genes of miR-350 did not include those previously reported  
125 to be associated with the pathophysiology of tumour cells.

126

127 **Fig 3. Comparison of the amounts of miR-350 (a), miR-671 (b), miR-22 (c), and**  
128 **miR-8865 (d) between exosomes and parent cells in the four cell lines.** The amount  
129 of miR-350 is significantly different between exosomes and parent cells, whereas those  
130 of miR-22, miR-671, and miR-8865 were not significantly different. All data represent  
131 the mean  $\pm$  SD of three independent experiments. \*P < 0.05.

132

### 133 **Exosomal protein profiles**

134 The results of separating exosomal proteins from each cell line by SDS-PAGE are  
135 shown in S5 Fig. Exosomal protein profiles were investigated by liquid  
136 chromatography-tandem mass spectrometry (LC-MS/MS). This analysis identified a  
137 total of 1,890 proteins among peptides extracted from exosomes of the four cell lines.

138 The top twenty proteins that were detected in each cell line by LC-MS/MS are  
139 listed in Table 2. As is the case with miRNAs, 13 proteins were commonly contained in  
140 the four cell lines. The abundantly contained proteins included those related to the  
141 cytoskeleton ( $\beta$ -actin and tubulins) and heat shock proteins. Except for these abundant

142 proteins, CD63 was detected in exosomes of all four cell lines and CD81 was detected  
 143 in those of CLBL-1, GL-1 and UL-1 among the exosome marker proteins, although  
 144 CD9 was not detected in any cell lines.  
 145

**Table 2. The top 20 proteins abundantly contained in exosomes in this study.**

CLBL-1	GL-1	UL-1	Ema
ACTB	ACTB	ACTB	ACTB
TUBB	TUBB	TUBB	TUBB
TUBB4B	TUBB4B	TUBB4B	TUBB4B
TUBB2B	TUBB2B	TUBB2B	TUBB2B
TUBB4A	TUBB4A	TUBB4A	TUBB4A
TUBA1C	TUBA1C	TUBA1C	TUBA1C
TUBA4A isoform X1	TUBA4A isoform X1	TUBA4A isoform X1	TUBA4A isoform X1
FLNA	FLNA	FLNA	FLNA
TLN1 isoform X4	TLN1 isoform X4	TLN1 isoform X4	TLN1 isoform X4
MYH9	MYH9	MYH9	MYH9
FAS	FAS	FAS	FAS
EEF2	EEF2	EEF2	EEF2
ACLY isoform X1	ACLY isoform X1	ACLY isoform X1	ACLY isoform X1
HSP90B	NCL	HSP90B	HSP90B
CCT2 isoform X1	IQGAP1	CCT2 isoform X1	CCT2 isoform X1
TUBBA3	DYNC1H1	DYNC1H1	DYNC1H1
CCT8 isoform X2	CLTC isoform X1	CLTC isoform X1	CLTC isoform X1
CCT8 isoform X1	GAPDH	GAPDH	GAPDH
CENP	CENP	EEF1A1	EEF1A1
HSP71	HSP71	EPRS isoform X1	PKM isoform X1

146

147 **Comparison of exosomal miRNA and protein profiles between**  
 148 **vincristine sensitive (VCR-S) cell lines and vincristine**

## 149 **resistant (VCR-R) cell lines**

150 The exosomal miRNA profiles were also compared between the VCR-S cell lines  
151 (CLBL-1 and GL-1) and the VCR-R cell line (UL-1) (see S6 Fig). In data from small  
152 RNA sequencing, the amounts of 11 miRNAs within exosomes were significantly lower  
153 in VCR-S cell lines than in the VCR-R cell line, and those of 5 miRNAs were  
154 significantly higher in VCR-S cell lines than in the VCR-R cell line ( $q < 0.01$ ). In parent  
155 cells, the amounts of 8 miRNAs were significantly lower in VCR-S cell lines than in the  
156 VCR-R cell line, and those of 7 miRNAs were higher in VCR-S cell lines than in the  
157 VCR-R cell line ( $q < 0.01$ ).

158 Among these miRNAs, the significant differences in the amounts of miR-151,  
159 miR-8908a-3p, and miR-486 were confirmed by RT-qPCR using the four cell lines  
160 including Ema, which is resistant to VCR (Fig 4). The amounts of miR-151 and  
161 miR-8908a-3p within exosomes and parent cells in VCR-S cell lines were significantly  
162 lower than those in VCR-R cell lines ( $P < 0.01$ ). The amount of miR-486 within  
163 exosomes and parent cells in VCR-S cell lines was significantly higher than those in  
164 VCR-R cell lines ( $P < 0.01$ ). The target genes were predicted for miR-151,  
165 miR-8908a-3p, and miR-486, and the top 10 target genes of each miRNA were  
166 extracted (see S2 Table). These genes included those that have been reported to be

167 associated with the biological behaviour of tumour cells (*NTRK2*, *MAPK8*, *BCOR*, and  
168 *PIK3R1* genes).

169

170 **Fig 4. Comparison of the amounts of miR-151 (a), miR-8908a-3p (b), and miR-486**  
171 **(c) between VCR-S and VCR-R cell lines.** The amounts of miR-151 and  
172 miR-8908a-3p in VCR-S cell lines were significantly lower than in VCR-R cell lines,  
173 and that of miR-486 in VCR-S cell lines were significantly higher than in VCR-R cell  
174 lines. All data represent the mean  $\pm$  SD of three independent experiments. \*P < 0.05.

175

176 Following the LC-MS/MS analysis, proteins that were detected only in VCR-S or  
177 VCR-R cell lines were also extracted (Table 3). Among these proteins, the difference in  
178 the amount of CD82 was validated by western blotting (Fig 5). CD82 was detected in  
179 exosomes of CLBL-1 and GL-1, while no band corresponding to CD82 was detected in  
180 exosomes of UL-1 and Ema. This protein was not detected in parent cells of all the four  
181 cell lines. HSP90B, which was selected as a protein that is abundantly contained in  
182 exosomes, was detected in exosomes from all four of the cell lines.

183

**Table 3. Exosomal proteins detected only in vincristine-sensitive or vincristine-resistant cell lines.**

Protein name	Total spectral count			
	CLBL-1	GL-1	UL-1	Ema
CD82	13	14	-	-
CD20 isoform X1	59	-	-	-
HLA-DRA	47	-	-	-
MHC class II beta	44	-	-	-
HLA-DQB	22	-	-	-
MHC class II	13	-	-	-
CD74 isoform X2	7	-	-	-
HLA-DQA	30	-	-	-
IGH constant region CH2	31	-	-	-
IGJ isoform X1	14	-	-	-
GZMK	-	-	23	59
PLOD1	-	-	14	36
HUWEI isoform X2	-	-	6	36
KLC1 isoform X8	-	-	8	14
HK2	-	-	60	13
DHX29	-	-	7	13
GANAB isoform X1	-	-	6	12
PWP1	-	-	5	10
EIF2B2	-	-	7	10
THOC2 isoform X1	-	-	8	9

-; not detected

185

186 **Fig 5. Western blotting for CD82 using proteins extracted from exosomes (a) and parent**  
187 **cells (b) of each cell line.** HSP90B and  $\beta$ -actin were selected for internal control for exosomes  
188 and parent cells, respectively. CD82 protein is detected in the exosomes of CLBL-1 and GL-1,  
189 whereas it was not detected in parent cells in any of the four cell lines. The figures of detection  
190 of CD82 within exosomes and parent cells were cropped from the different parts of the same  
191 figure of the membrane. The figures of HSP90B and  $\beta$ -actin were cropped from the figures of the  
192 different membrane. The full-length figures of blotting membrane are shown in S7 Fig.

193

## 194 **Discussion**

195 In the present study, the miRNA and protein profiles within exosomes derived from four  
196 canine lymphoid tumour cell lines were comprehensively analysed by small RNA sequencing  
197 and LC-MS/MS.

198 In small RNA sequencing, the mapping rate of the reads to canine miRNA was  
199 comparatively lower in both exosomes and parent cells of Ema than the other three cell lines. In  
200 the hierarchical clustering analysis and PCA plots for three cell lines, three distinct clusters  
201 composed of the exosomes and parent cells of each cell line were observed. Therefore, it was

202 indicated that miRNA profiles within exosomes reflect those of parent cells and the profiles of  
203 exosomal miRNA varied among cell lines.

204 Small RNA sequencing also revealed that five miRNAs (let-7f, let-7g, miR-7, miR-30d,  
205 and miR-92a) were abundantly contained both in exosomes and parent cells of all four of the cell  
206 lines. Previous studies have reported that exosomes derived from tumour cells contain miRNAs  
207 of the let-7 family [17,18]. It has also been reported that miR-30d and miR-92a are abundant in  
208 exosomes of Gamma-Herpesvirus-infected lymphoma cell lines [12]. Therefore, these miRNAs  
209 might be associated with the pathophysiology of lymphoid tumours, and further studies are  
210 needed to reveal the biological roles of these miRNAs in exosomes derived from tumour cells.

211 In the comparison of the amounts of miRNAs between exosomes and parent cells,  
212 significant differences were observed for 39, 20, and 24 miRNAs in CLBL-1, UL-1, and Ema,  
213 respectively, whereas there was no significant difference in GL-1. Among these miRNAs, the  
214 significant differences in the amounts of miR-350 between exosomes and parent cells were  
215 confirmed in all four cell lines by RT-qPCR. The predicted target genes of miR-350 did not  
216 include those previously reported to be associated with the pathophysiology of tumour cells.  
217 However, miR-350 was reported to promote apoptosis through down-regulation of *PIK3R3* gene  
218 [19]. Further studies are needed to reveal the functions of miR-350 in the microenvironmental

219 crosstalk in lymphoma.

220 LC-MS/MS analysis revealed that exosomes derived from each cell line contain various  
221 types of protein. Most of the proteins abundantly contained in exosomes were common among  
222 the four cell lines, including those related to cytoskeleton, such as  $\beta$ -actin, tubulins, and heat  
223 shock proteins. In addition, CD63 or CD81 were also detected in exosomes derived from each  
224 cell line. Exosomal markers have been reported to include members of the tetraspanin family  
225 (CD9, CD63, and CD81) and heat shock proteins (HSP60, HSP70, and HSP90) [20,21]. It was  
226 also reported that exosomes derived from Jurkat cells contain  $\beta$ -actin and tubulins [22]. Thus,  
227 those results in previous studies are consistent with those in the present study.

228 In the comparison of the amounts of miRNA within the exosomes, the amounts of  
229 miR-151, miR-8908a-3p, and miR-486 were confirmed to be different between VCR-S cell lines  
230 and VCR-R cell lines by RT-qPCR. The amounts of miR-151 and miR-8908a-3p were  
231 significantly lower in VCR-S cell lines, while miR-486 was significantly more abundant in these  
232 cell lines. The target genes of miR-151 included the gene *NTRK2*, a member of neurotrophic  
233 tyrosine receptor kinase family. The expression of *NTRK2* was reported to be down-regulated in  
234 patients with breast cancer with a poor prognosis [23]. The expression of this gene was also  
235 reported to suppress anoikis by activating the PI3K/Akt pathway in human ovarian cancer cells



236 [24]. The target genes of miR-8908a-3p included *MAPK8* (also known as *JNK1*) and *BCOR*. The  
237 *MAPK8* gene is a member of the MAP kinase and JNK family, and involved in various cellular  
238 processes including cell proliferation, differentiation, and apoptosis [25,26]. The *BCOR* gene  
239 encodes a co-repressor of BCL6, a transcriptional repressor that is required for formation of  
240 germinal centres [27,28] and silences various genes involved in the cell cycle and apoptosis [29].  
241 The target genes of miR-486 included *PIK3R1*, one of the oncogenes that promotes cell  
242 proliferation and tumour cell invasion [30]. Based on this evidence, it is possible that these  
243 miRNAs might be associated with the resistance to VCR in lymphoid tumours. Further studies  
244 are needed to elucidate the association of these miRNAs with drug resistance and  
245 microenvironmental crosstalk in lymphoid tumours.

246       Among the proteins detected by LC-MS/MS in the present study, CD82 were detected in  
247 the exosomes of VCR-S cell lines but not in those of VCR-R cell lines, and the difference in its  
248 amount was confirmed by western-blotting. In addition, CD82 was not detected in proteins  
249 extracted from parent cells of CLBL-1 and GL-1, suggesting that CD82 was selectively delivered  
250 into exosomes in these cell lines. CD82 has been reported to suppress tumour metastasis [31] and  
251 be associated with tumour cell growth [32] and survival [33]. Therefore, it is possible that CD82  
252 expression in exosomes might be associated with the biological behaviour of tumour cells,

253 including metastasis, tumour growth, cell survival, and drug sensitivity, via its function in  
254 microenvironmental crosstalk in lymphoid tumours. Further studies are needed to investigate the  
255 biological roles of CD82 in microenvironmental crosstalk in lymphoid tumours.

256 In conclusion, most of the miRNAs and proteins abundantly contained in exosomes are  
257 common among the four cell lines, but the miRNA profiles in exosomes reflect those of parent  
258 cells and differ among cell lines. In addition, miR-151, miR-8908a-3p, miR-486, and CD82  
259 proteins were differentially abundant within the exosomes between VCR-S and VCR-R cell  
260 lines. Further investigations are needed to elucidate the biological functions of these molecules in  
261 the crosstalk between tumour cells and tumour microenvironment.

262

## 263 **Materials and methods**

### 264 **Cell lines and cell culture**

265 Four canine lymphoid tumour cell lines (CLBL-1, GL-1, UL-1, and Ema) were used in this  
266 study: CLBL-1, a canine B-cell lymphoma cell line [34]; GL-1, a canine B-cell leukaemia cell  
267 line [35]; UL-1, a canine T-cell lymphoma cell line [36]; and Ema; a canine T-cell lymphoma  
268 cell line [37]. UL-1 and Ema were established from dogs with lymphoma showing drug  
269 resistance after chemotherapy, whereas CLBL-1 and GL-1 were established from dogs with

270 leukaemia or lymphoma who were not subjected to chemotherapy. CLBL-1, GL-1, and Ema  
271 were kindly provided by Dr. Rütgen, University of Veterinary Medicine Vienna, Austria, Dr.  
272 Nakaichi, Yamaguchi University, Japan, and Dr. Mizuno, Yamaguchi University, Japan,  
273 respectively. Our group established UL-1 previously [36]. Our previous study reported that  
274 CLBL-1 and GL-1 were sensitive to vincristine, and UL-1 and Ema were resistant to vincristine  
275 [38]. These cell lines were cultured in RPMI-1640 medium at 37°C, with 10% foetal bovine  
276 serum (Biowest, Nuaille, France) in a humidified atmosphere containing 5% CO<sub>2</sub>.

277

## 278 **Exosome isolation and preparation of total RNA and protein of** 279 **exosomes and parent cells**

280 Exosomes were isolated from  $3 \times 10^7$  cells (CLBL-1, GL-1, and UL-1) and  $2 \times 10^7$  cells  
281 (Ema) cultured for 24h in growth medium without foetal bovine serum. Exosomes were isolated  
282 from cell culture media using the Total Exosome Isolation (from cell culture media)  
283 (ThermoFisher Scientific, Waltham, MA, USA), and exosome protein and RNA were prepared  
284 using the Total Exosome RNA and Protein Isolation Kit (ThermoFisher Scientific) according to  
285 the manufacturer's instructions. The number and sizes of isolated exosomes were measured  
286 using NanoSight NS300 system (Malvern Instruments, Malvern, UK). The concentrations of

287 exosome protein samples were measured using Micro BCA Protein Assay (ThermoFisher  
288 Scientific), and the concentrations and size distributions of exosomal RNA samples were  
289 measured using Agilent RNA 6000 Pico Kit and Agilent 2100 Bioanalyzer (Agilent  
290 Technologies, Palo Alto, CA, USA). Total RNA of each parent cell line was extracted using  
291 miRNeasy Mini Kit (QIAGEN, Limburg, Netherlands), and concentration and integrity were  
292 measured as described above. Each total RNA sample was prepared in duplicate.

293

## 294 **Small RNA sequencing and data processing**

295 Small RNA sequencing libraries were prepared with 156 ng of total RNA using NEB Next  
296 Multiplex Small RNA Library Prep Kit (New England Biolabs, Ipswich, MA, USA). RNA  
297 sequencing was performed in duplicate using NextSeq500 (Illumina, San Diego, CA, USA) with  
298 High Output Kit (Illumina) as stranded, single 36-base reads following the manufacturer's  
299 instruction.

300 Raw BCL data for each sample were de-multiplexed with bcl2fastq (version 2.18.0.12)  
301 and were stored in independent FASTQ files. The sequence data were trimmed with  
302 Trimomatic (version 0.36) [39] to clean up sequences with low-quality and those with  
303 sequencing adaptors. After trimming, a subset of short reads was aligned to cfa\_MiR\_453

304 (<http://www.targetscan.org/>) with Bowtie2 (version 2.2.9) [40]. The depth of the reads aligned to  
305 cfa\_MiR\_453 was quantified using Samtools (version 1.3.1). Counts per million (CPM) was  
306 imported into R (version 3.3.2) and principal component analysis was conducted. Then, miRNA  
307 counts for each sample were imported into R for differential expression analysis with EdgeR  
308 [41,42]. Cluster3.0 and Java Treeview (version 1.1.6r4) were used for hierarchical clustering and  
309 visualization. The data from small RNA sequencing in this study are available in the DDBJ  
310 Sequenced Read Archive database with the accession number DRA006696.

311

## 312 **Quantitative real-time RT-PCR**

313 The amounts of miRNAs extracted from the small RNA sequencing data were validated by  
314 RT-qPCR using TaqMan MicroRNA Assay (Applied Biosystems, Foster City, CA, USA). The  
315 candidate miRNAs selected for validation are listed in the Supplementary Table S3 online.  
316 Briefly, 3.3 ng of total RNA was reverse transcribed using TaqMan MicroRNA Reverse  
317 Transcription Kit (Applied Biosystems), and qPCR was performed using TaqMan MicroRNA  
318 Assay and Thermal Cycler Dice Real Time System TP800 (Takara Bio, Shiga, Japan). Data were  
319 expressed as mean  $C_T$  values of three independent experiments performed in triplicate.  $C_T$  values  
320 were determined using the second derivative maximum method, in which a  $C_T$  value is expressed

321 as the cycle number at which the second derivative was at its maximum. After validation, target  
322 genes of the miRNAs were predicted using miRbase (<http://www.mirbase.org/>) [43,44].

323

## 324 **LC-MS/MS**

325 Protein profiles of exosomes were analysed by LC-MS/MS. An EASY-Spray column (15  
326 cm × 75 µm I.D., 3 µm, ThermoFisher Scientific) was employed for separation of each exosomal  
327 protein sample at the flow rate of 300 nl/min. A quadrupole tandem mass spectrometer (Q  
328 Exactive Plus, ThermoFisher Scientific) was used in positive ion mode for analytic detection.  
329 The raw MS spectra data were queried against the NCBI Canine protein sequence database using  
330 the MASCOT database search engine, and peptides were quantified according to the spectral  
331 counts.

332

## 333 **Western-blotting**

334 Expressions of the candidate proteins extracted from the LC-MS/MS data were verified by  
335 western blotting. One µg of protein extracted from exosome or parent cells was separated by  
336 SDS-PAGE and blotted onto a PVDF membrane. The membranes were blocked in 5% skimmed  
337 milk and incubated with primary antibodies against CD82, HSP90B, or β-actin. HSP90B was

338 selected as the internal control of the exosomal protein. Then, the membranes were incubated  
339 with secondary antibodies. The antibodies, dilutions, and incubation temperatures are shown in  
340 the Supplementary Table S4 online. After incubation, positive immunoreactivity was detected  
341 using Luminata Forte Western HRP Substrate (Merck Millipore, Darmstadt, Germany) and  
342 visualized using a ChemiDoc XRS Plus (Bio-Rad Laboratories, Hercules, CA, USA).

343

## 344 **Statistical analysis**

345 In the differential expression analysis using EdgeR, a false discovery rate (q-value) of less  
346 than 0.01 was considered statistically significant. One-way ANOVA followed by Tukey's  
347 post-hoc test was performed for multiple comparisons of miRNA quantities in the RT-qPCR  
348 using the STATMATE (ATMS, Tokyo, Japan) software, and P-values of less than 0.05 were  
349 considered statistically significant.

350

## 351 **References**

- 352 1 Zoller M. Janus-faced myeloid-derived suppressor cell exosomes for the good and the  
353 bad in cancer and autoimmune disease. *Front Immunol.* 2011;9: 137.
- 354 2 Bebelman MP, Smit MJ, Pegtel DM, Baglio SR. Biogenesis and function of extracellular  
355 vesicles in cancer. *Pharmacol Ther.* 2018 S0163-7258(18)30038-X.
- 356 3 Dai G, Yao X, Zhang Y, Gu J, Geng Y, Xue F, et al. Colorectal cancer cell-derived  
357 exosomes containing miR-10b regulate fibroblast cells via the PI3K/Akt pathway. *Bull*  
358 *Cancer.* 2018;105: 336-349.

359 4 Piao YJ, Kim HS, Hwang EH, Woo J, Zhang M, Moon WK. Breast cancer cell-derived  
360 exosomes and macrophage polarization are associated with lymph node metastasis.  
361 *Oncotarget*. 2018;9: 7398-7410.

362 5 Bardi GT, Smith MA, Hood JL. Melanoma exosomes promote mixed M1 and M2  
363 macrophage polarization. *Cytokine*. 2018;105: 63-72.

364 6 An M, Zhu J, Wu J, Cuneo KC, Lubman DM. Circulating exosomes from pancreatic  
365 cancer accelerate the migration and proliferation of PANC-1 cells. *J Proteome Res*.  
366 2018;17: 1690-1699.

367 7 Yang YZ, Zhang XY, Fang LJ, Wan Q, Li J. Role of exosomes in the cross-talk between  
368 leukemia cells and mesenchymal stem cells -Review. *Zhongguo Shi Yan Xue Ye Xue Za*  
369 *Zhi*. 2017;25: 1255-1258.

370 8 Xu B, Wang T. Intimate cross-talk between cancer cells and the tumor microenvironment  
371 of B-cell lymphomas: The key role of exosomes. *Tumour Biol*. 2017;39:  
372 1010428317706227.

373 9 Hedlund M, Nagaeva O, Kargl D, Baranov V, Mincheva-Nilsson L. Thermal- and  
374 oxidative stress causes enhanced release of NKG2D ligand-bearing immunosuppressive  
375 exosomes in leukemia/lymphoma T and B cells. *PLoS One*. 2011;6: e16899.

376 10 Min QH, Wang XZ, Zhang J, Chen QG, Li SQ, Liu XQ, et al. Exosomes derived from  
377 imatinib-resistant chronic myeloid leukemia cells mediate a horizontal transfer of  
378 drug-resistant trait by delivering miR-365. *Exp Cell Res*. 2018;362: 386-393.

379 11 Wang J, Li D, Zhuang Y, Fu J, Li X, Shi Q, et al. Exosomes derived from bone marrow  
380 stromal cells decrease the sensitivity of leukemic cells to etoposide. *Oncol Lett*. 2017;14:  
381 3082-3088.

382 12 Hoshina S, Sekizuka T, Kataoka M, Hasegawa H, Hamada H, Kuroda M, et al. Profile of  
383 exosomal and intracellular microRNA in gamma-herpesvirus-infected lymphoma cell  
384 lines. *PLoS One*. 2016;11: e0162574.

385 13 Yeh YY, Ozer HG, Lehman AM, Maddocks K, Yu L, Johnson AJ, et al. Characterization  
386 of CLL exosomes reveals a distinct microRNA signature and enhanced secretion by  
387 activation of BCR signaling. *Blood*. 2015;125: 3297-3305.

388 14 Tamaru JI. 2016 revision of the WHO classification of lymphoid neoplasms. *Rinsho*  
389 *ketsueki*. 2017;58: 2188-2193.

390 15 Seelig DM, Avery AC, Ehrhart EJ, Linden MA. The comparative diagnostic features of  
391 canine and human lymphoma. *Vet Sci*. 2016;3: pii: 11.

392 16 Villarnovo D, McCleary-Wheeler AL, Richards KL. Barking up the right tree: advancing  
393 our understanding and treatment of lymphoma with a spontaneous canine model. *Curr*



394 Opin Hematol. 2017;24: 359-366.

395 17 Ohshima K, Inoue K, Fujiwara A, Hatakeyama K, Kanto K, Watanabe Y, et al. Let-7  
396 microRNA family is selectively secreted into the extracellular environment via exosomes  
397 in a metastatic gastric cancer cell line. PLoS One. 2010;5: e13247.

398 18 Liao J, Liu R, Yin L, Pu Y. Expression profiling of exosomal miRNAs derived from  
399 human esophageal cancer cells by Solexa high-throughput sequencing. Int J Mol Sci.  
400 2014;15: 15530-15551.

401 19 Sui J, Fu Y, Zhang Y, Ma S, Yin L, Pu Y, et al. Molecular mechanism for miR-350 in  
402 regulating of titanium dioxide nanoparticles in macrophage RAW264.7 cells. Chem Biol  
403 Interact. 2018;280: 77-85.

404 20 Simpson RJ, Lim JW, Moritz RL, Mathivanan S. Exosomes: proteomic insights and  
405 diagnostic potential. Expert Rev Proteomics. 2009;6: 267-283.

406 21 Yoshioka Y, Konishi Y, Kosaka N, Katsuda T, Kato T, Ochiya T. Comparative marker  
407 analysis of extracellular vesicles in different human cancer types. J Extracell Vesicles.  
408 2013;2: 20424.

409 22 Bosque A, Dietz L, Gallego-Lleyda A, Sanclemente M, Iturralde M, Naval J, et al.  
410 Comparative proteomics of exosomes secreted by tumoral Jurkat T cells and normal  
411 human T cell blasts unravels a potential tumorigenic role for valosin-containing protein.  
412 Oncotarget. 2016;7: 29287-29305.

413 23 Li Z, Peng L, Han S, Huang Z, Shi F, Cai Z, et al. Screening molecular markers in early  
414 breast cancer of the same pathological types but with different prognoses using Agilent  
415 gene chip. Nan Fang Yi Ke Da Xue Xue Bao. 2013;33: 1483-1488.

416 24 Yu X, Liu L, Cai B, He Y, Wan X. Suppression of anoikis by the neurotrophic receptor  
417 TrkB in human ovarian cancer. Cancer Sci. 2008;99: 543-552.

418 25 Cantley LC. The phosphoinositide 3-kinase pathway. Science. 2002;296: 1655-1657.

419 26 Wada T, Penninger JM. Mitogen-activated protein kinases in apoptosis regulation.  
420 Oncogene. 2004;23: 2838-2849.

421 27 Ci W, Polo JM, Melnick A. B-cell lymphoma 6 and the molecular pathogenesis of diffuse  
422 large B-cell lymphoma. Curr Opin Hematol. 2008;15: 381-390.

423 28 Hatzi K, Jiang Y, Huang C, Garret-Bakelman F, Gearhart MD, Giannopoulou EG, et al.  
424 A hybrid mechanism of action for BCL6 in B cells defined by formation of functionally  
425 distinct complexes at enhancers and promoters. Cell Rep. 2013;4: 578-588.

426 29 Cardenas MG, Oswald E, Yu W, Xue F, MacKerell AD Jr, Melnick AM. The expanding  
427 role of the BCL6 oncoprotein as a cancer therapeutic target. Clin Cancer Res. 2017;23:  
428 885-893.

429 30 He S, Zhang J, Zhang W, Chen F, Luo R. FOXA1 inhibits hepatocellular carcinoma  
430 progression by suppressing PIK3R1 expression in male patients. *J Exp Clin Cancer Res.*  
431 2017;36: 175.

432 31 Zoller M. Tetraspanins: push and pull in suppressing and promoting metastasis. *Nat Rev*  
433 *Cancer* 2009;9: 40-55.

434 32 Yang X, Wei LL, Tang C, Slack R, Mueller S, Lippman ME. Overexpression of KAI1  
435 suppresses in vitro invasiveness and in vivo metastasis in breast cancer cells. *Cancer Res.*  
436 2001;61: 5284-5288.

437 33 Tohami T, Drucker L, Shapiro H, Radnay J, Lishner M. Overexpression of tetraspanins  
438 affects multiple myeloma cell survival and invasive potential. *Faseb J.* 2007;21: 691-699.

439 34 Rutgen BC, Hammer SE, Gerner W, Christian M, de Arespacochaga AG, Willmann M,  
440 et al. Establishment and characterization of a novel canine B-cell line derived from a  
441 spontaneously occurring diffuse large cell lymphoma. *Leuk Res.* 2010;34: 932-938.

442 35 Nakaichi M, Taura Y, Kanki M, Mamba K, Momoi Y, Tsujimoto H, et al. Establishment  
443 and characterization of a new canine B-cell leukemia cell line. *J Vet Med Sci.* 1996;58:  
444 469-471.

445 36 Yamazaki J, Baba K, Goto-Koshino Y, Setoguchi-Mukai A, Fujino Y, Ohno K, et al.  
446 Quantitative assessment of minimal residual disease (MRD) in canine lymphoma by  
447 using real-time polymerase chain reaction. *Vet Immunol Immunopathol.* 2008;126:  
448 321-331.

449 37 Hiraoka H, Minami K, Kaneko N, Shimokawa-Miyama T, Okamura Y, Mizuno T, et al.  
450 Aberrations of the FHIT gene and Fhit protein in canine lymphoma cell lines. *J Vet Med*  
451 *Sci.* 2009;71: 769-777.

452 38 Tomiyasu H, Goto-Koshino Y, Fujino Y, Ohno K, Tsujimoto H. Epigenetic regulation of  
453 the ABCB1 gene in drug-sensitive and drug-resistant lymphoid tumour cell lines obtained  
454 from canine patients. *Vet J.* 2014;199: 103-109.

455 39 Bolger AM, Lohse M, Usadel B. Trimmomatic: a flexible trimmer for Illumina sequence  
456 data. *Bioinformatics.* 2014;30: 2114-2120.

457 40 Langmead B, Salzberg SL. Fast gapped-read alignment with Bowtie 2. *Nat Methods.*  
458 2012;9: 357-359.

459 41 Robinson MD, McCarthy DJ, Smyth GK. edgeR: a Bioconductor package for differential  
460 expression analysis of digital gene expression data. *Bioinformatics.* 2010;26: 139-140.

461 42 Zhou X, Lindsay H, Robinson MD. Robustly detecting differential expression in RNA  
462 sequencing data using observation weights. *Nucleic Acids Res.* 2014;42: e91.

463 43 Kozomara A, Griffiths-Jones S. miRBase: annotating high confidence microRNAs using

464 deep sequencing data. Nucleic Acids Res. 2014;42: D68-73.  
465 44 Kozomara A, Griffiths-Jones S. miRBase: integrating microRNA annotation and  
466 deep-sequencing data. Nucleic Acids Res. 2011;39: D152-157.  
467

## 468 **Supporting information**

469 **S1 Table. The mean numbers of raw reads, reads mapped to miRNA, and the mapping**  
470 **rates to miRNA.**

471 **S2 Table. The top 10 predicted target genes of miRNAs extracted in this study.**

472 **S3 Table. miRNAs extracted for validation by RT-qPCR and TaqMan MicroRNA Assay**  
473 **IDs for these miRNAs.**

474 **S4 Table. Primary and secondary antibodies for detection of CD82, HSP90B, and  $\beta$ -actin.**

475 **S1 Fig. The size distributions of exosomes isolated from CLBL-1 (a), GL-1 (b), UL-1 (c),**  
476 **and Ema (d).**

477 **S2 Fig. The RNA integrity numbers (RINs) and size distributions of total RNA samples**  
478 **derived from exosomes and parent cells in CLBL-1 (a), GL-1 (b), UL-1 (c), and Ema (d).**

479 “18S” indicates the peak of 18S ribosomal RNA, and “28S” indicates that of 28S ribosomal  
480 RNA.

481 **S3 Fig. PCA plots analysis including data of Ema cell line. Exosomes and parent cells**  
482 clustered similarly for each cell line and the profiles are different among cell lines. Orange dots

483 (exosomes) and red dots (parent cells) correspond to CLBL-1, violet dots (exosomes) and blue  
484 dots (parent cells) to GL-1, grey dots (exosomes) and black dots (parent cells) to UL-1, and  
485 yellow dots (exosomes) and green dots (parent cells) to Ema.

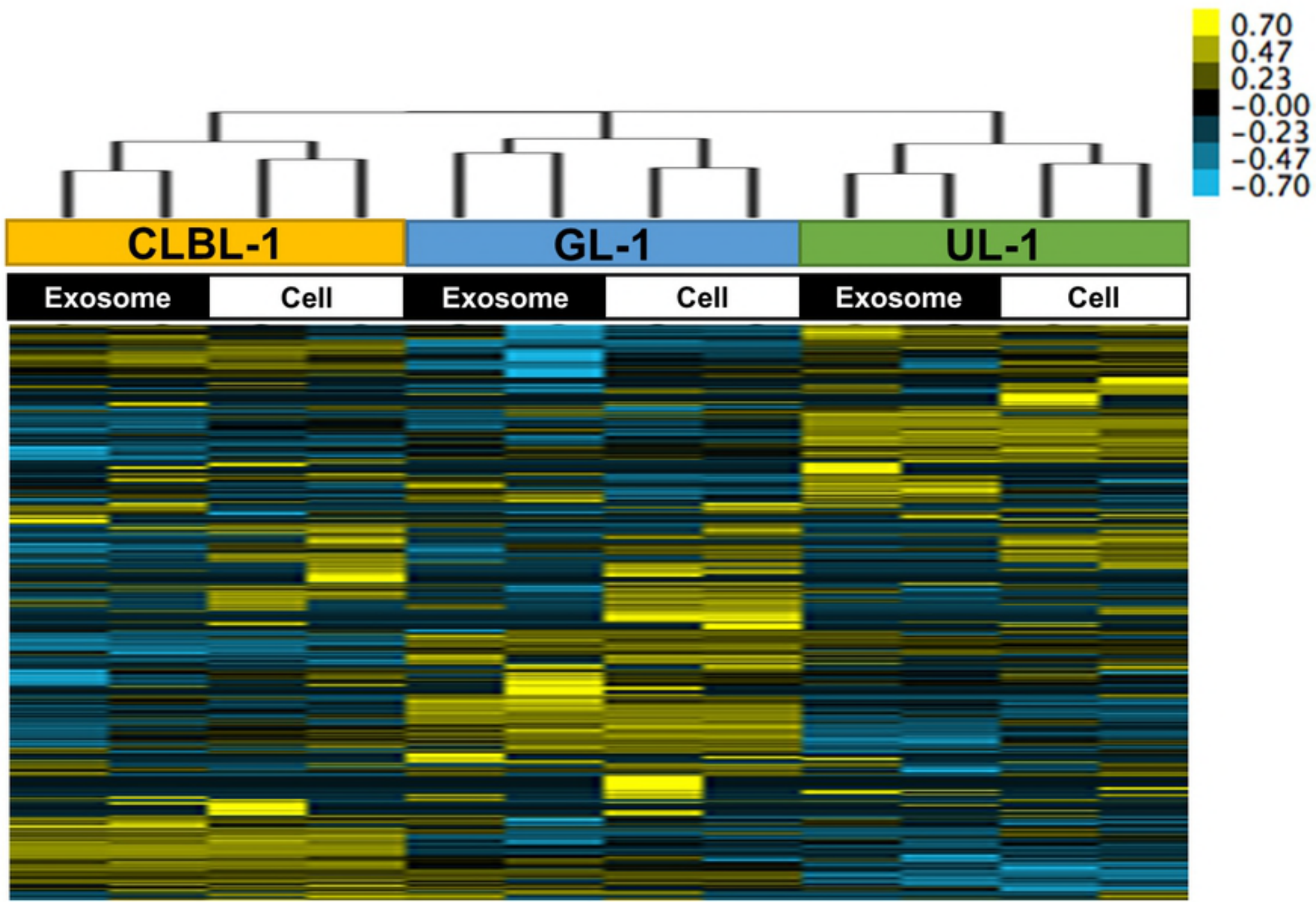
486 **S4 Fig. The Venn diagram showing the common miRNAs whose amounts were significantly**  
487 **different between exosomes and parent cells in small RNA sequencing.** The names of  
488 miRNAs that were significantly more abundant in exosomes than parent cells are shown in red,  
489 and those that were significantly less abundant in exosomes than parent cells are shown in blue.

490 **S5 Fig. The separation of exosomal proteins from each cell line by SDS-PAGE.** Lane M is  
491 the protein ladder. Lanes 1-4 correspond to the exosomal protein from CLBL-1, GL-1, UL-1, and  
492 Ema, respectively, and lanes 1'-4' correspond to exosomal protein precipitated with  
493 trichloroacetic acid from CLBL-1, GL-1, UL-1, and Ema, respectively.

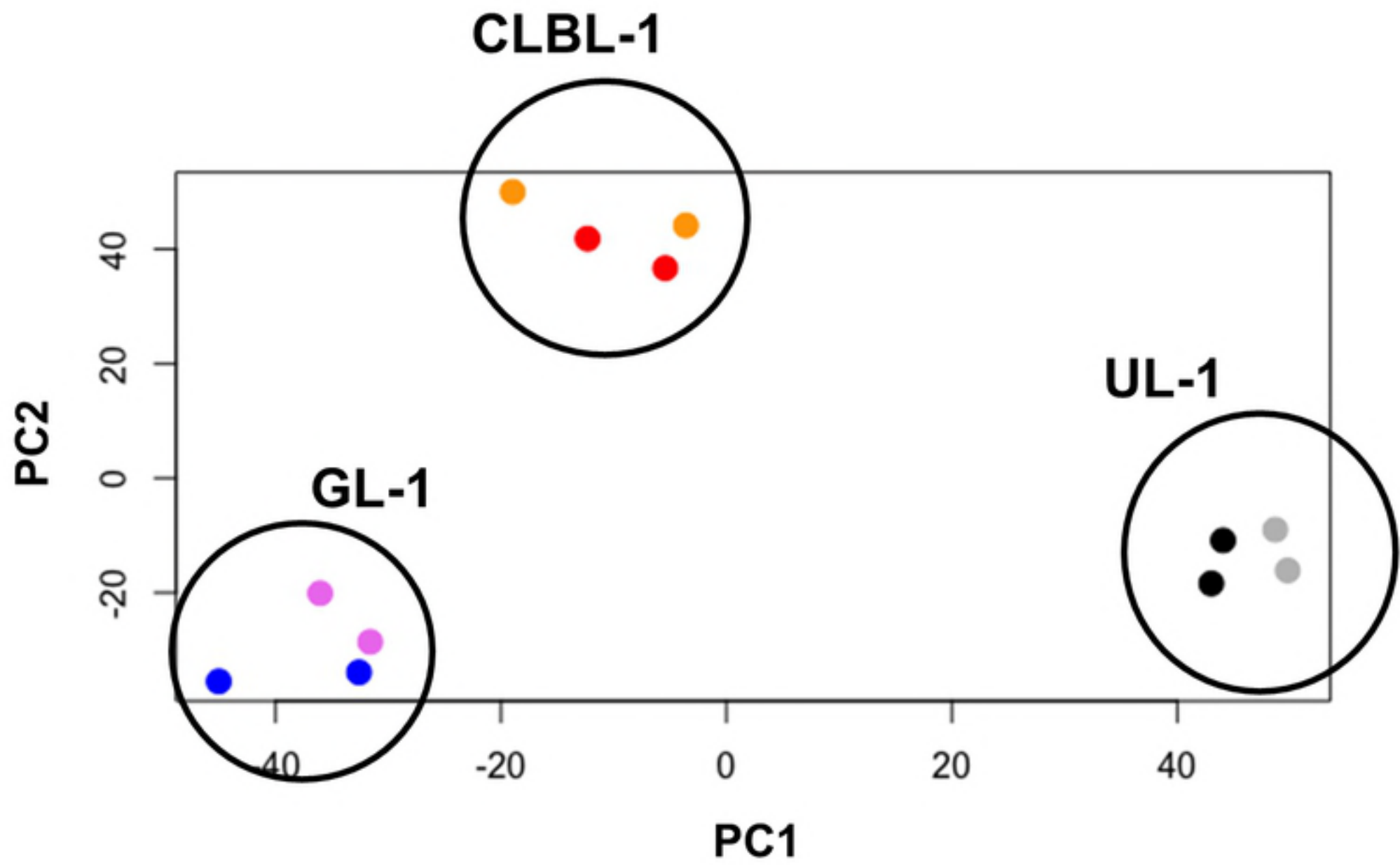
494 **S6 Fig. Heat maps showing the miRNAs whose amounts were significantly different**  
495 **between VCR-S cell lines and the VCR-R cell line in exosomes (a) and cells (b).** In  
496 exosomes, the amounts of 11 miRNAs were significantly lower in VCR-S cell lines than in the  
497 VCR-R cell line, and those of 5 miRNAs were significantly higher in VCR-S cell lines than in  
498 the VCR-R cell line. In parent cells, the amounts of 8 miRNAs were significantly lower in

499 VCR-S cell lines than in the VCR-R cell line, and those of 7 miRNAs were higher in VCR-S cell  
500 lines than in the VCR-R cell line.

501 **S7 Fig. Full-length figures of blotting membrane that were used for the detection of CD82**  
502 **(a, b), HSP90B (c), and  $\beta$ -actin (d) by Western blotting.** The figures of the same membrane  
503 were shown in (a) and (b), but exposure time was different between these figures. In Fig 5, the  
504 figures of detection of CD82 within exosomes and parent cells were cropped from the different  
505 parts of (b). The figures of detection of HSP90B and  $\beta$ -actin were cropped from (c) and (d),  
506 respectively.



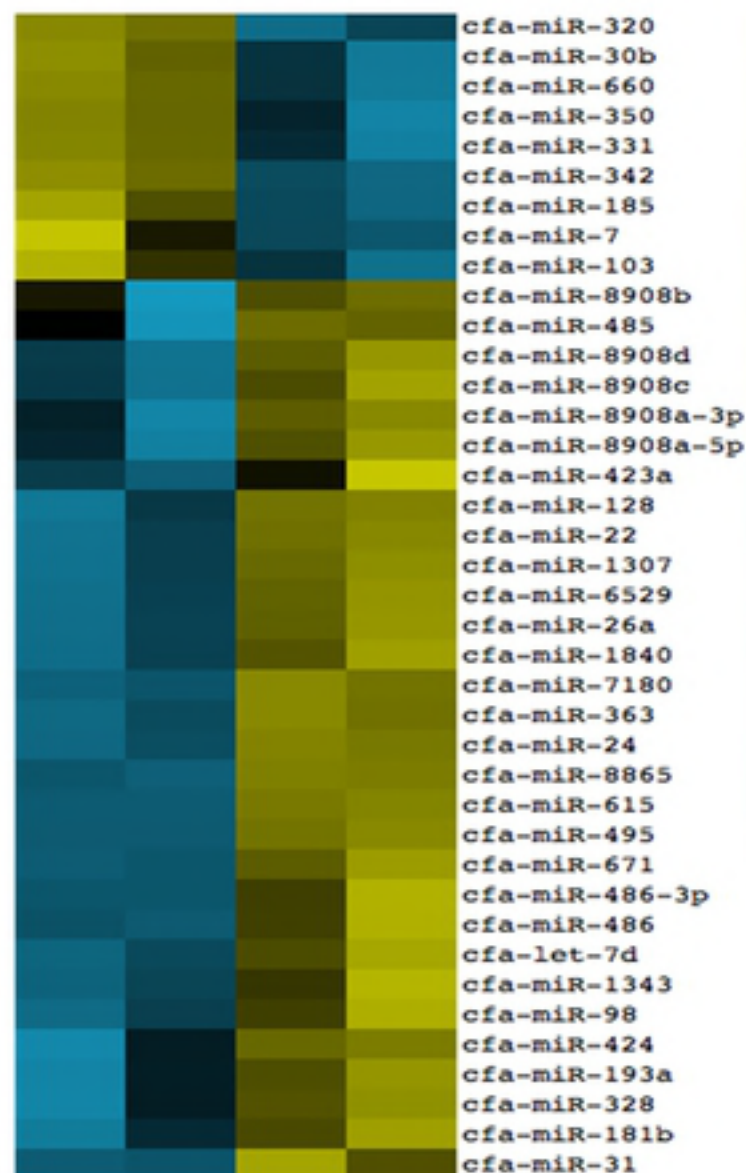
Figure



Figure

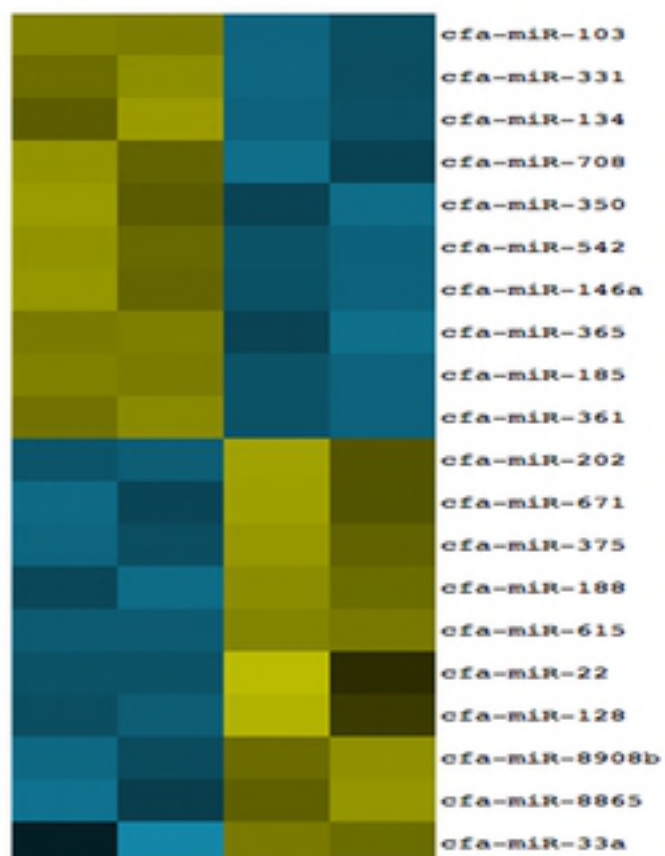
### (a) CLBL-1

Exosome Cell



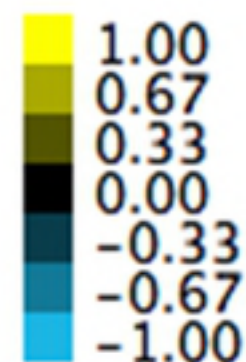
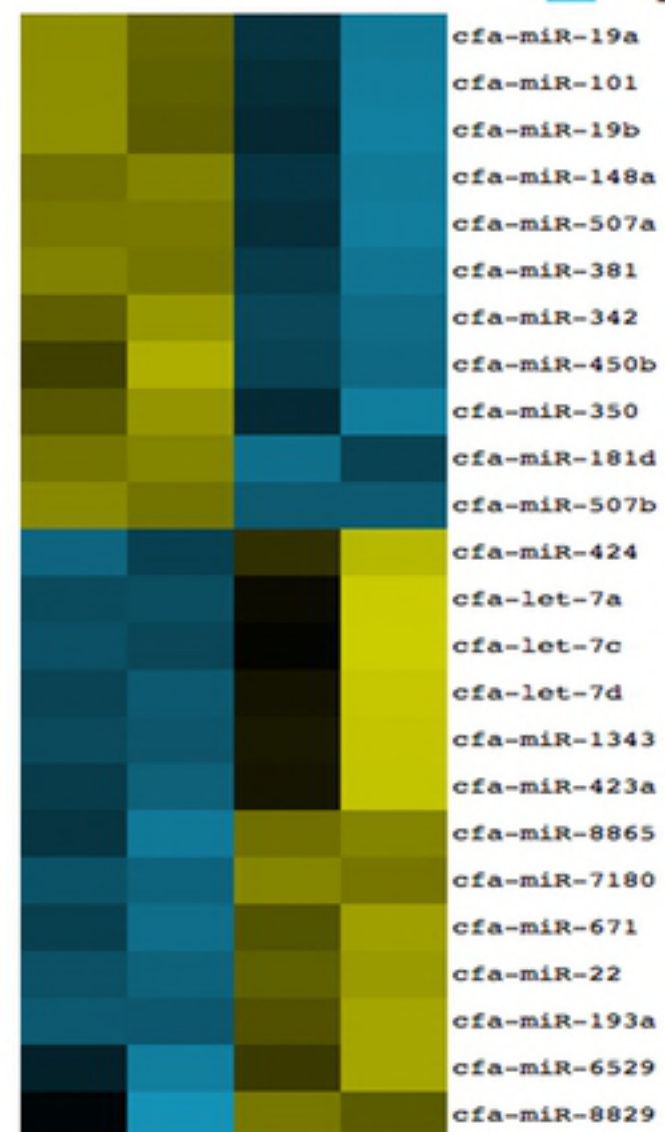
### (b) UL-1

Exosome Cell



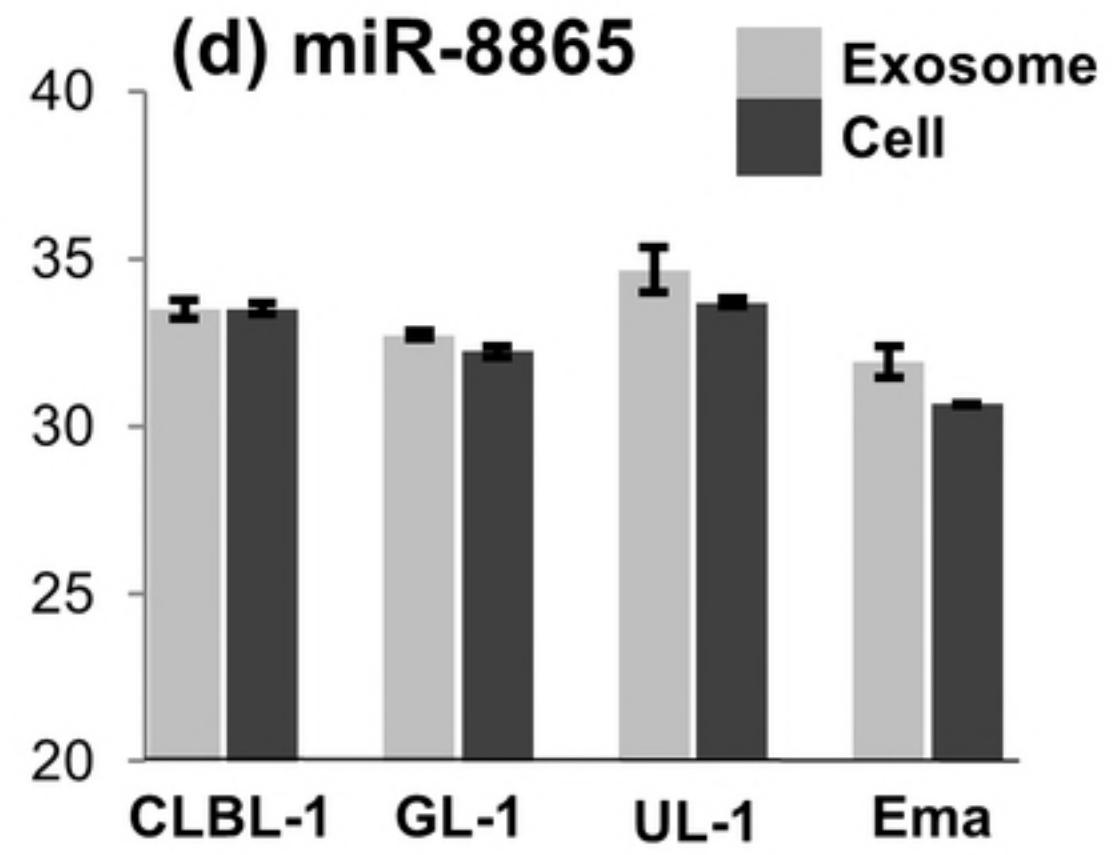
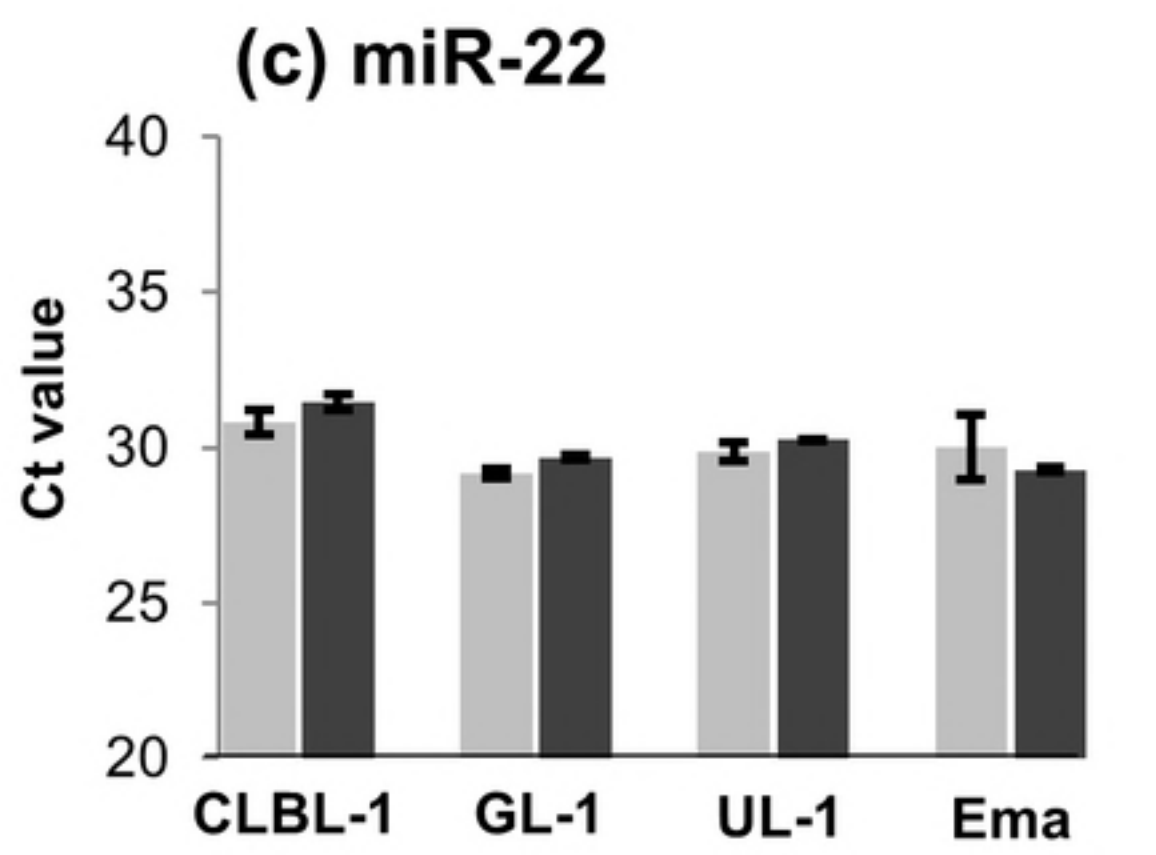
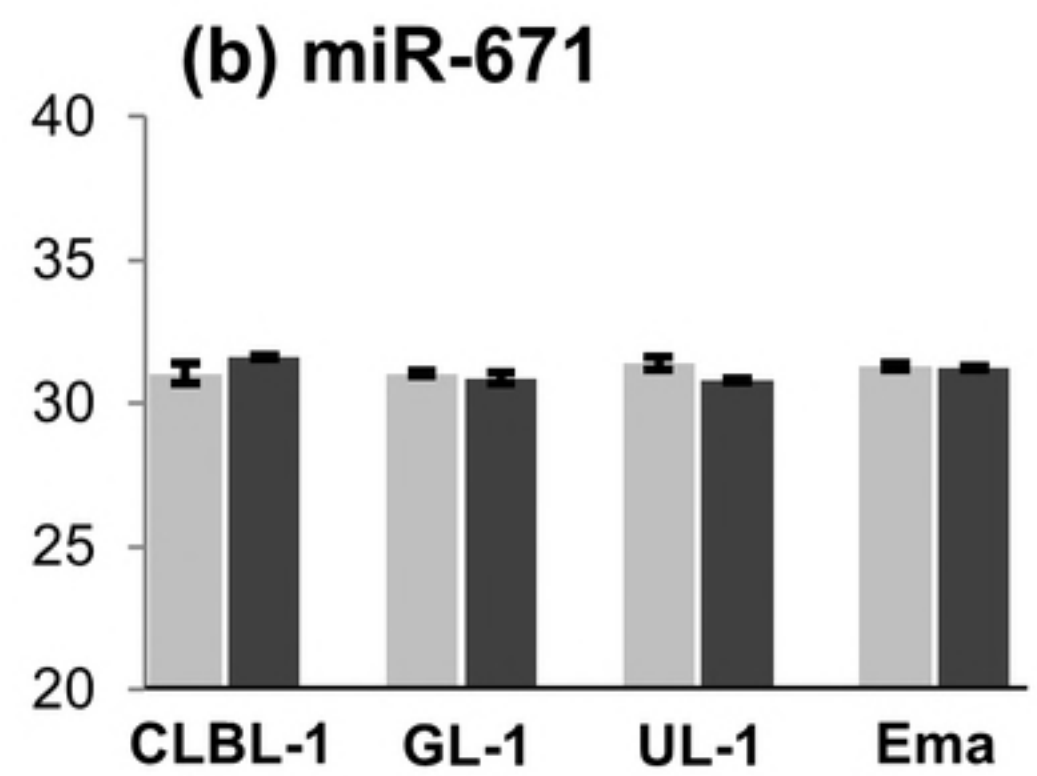
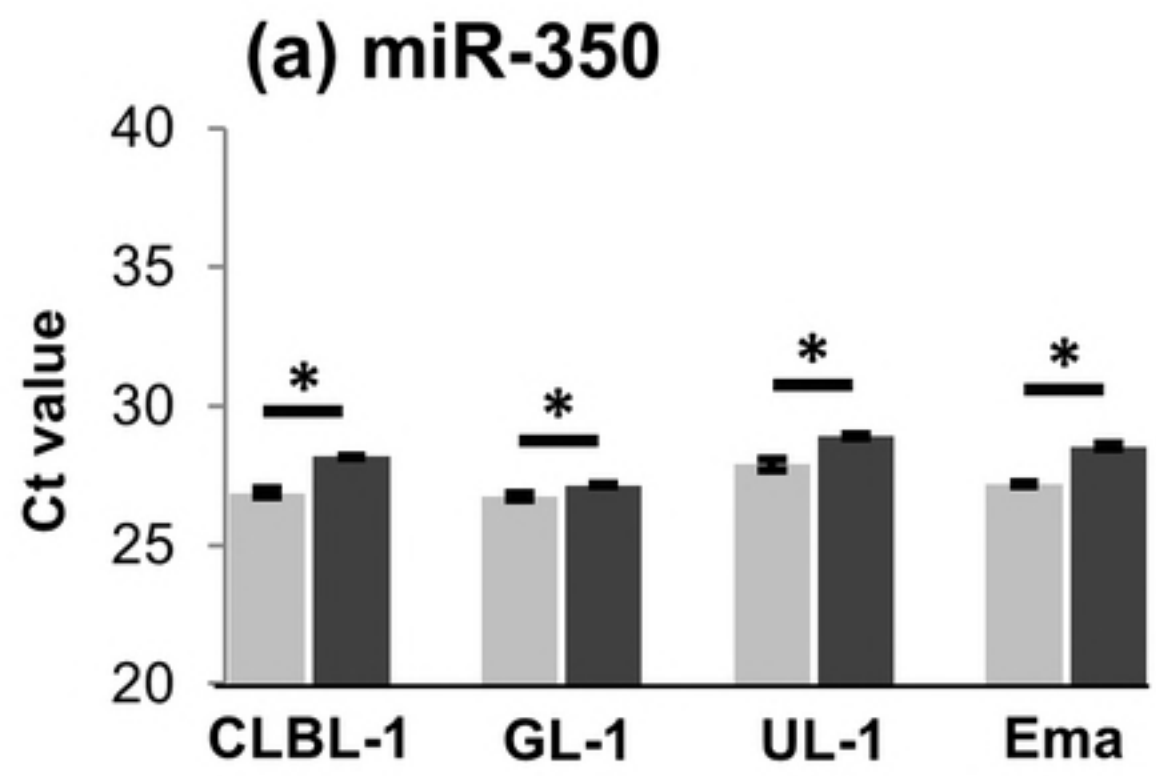
### (c) Ema

Exosome Cell



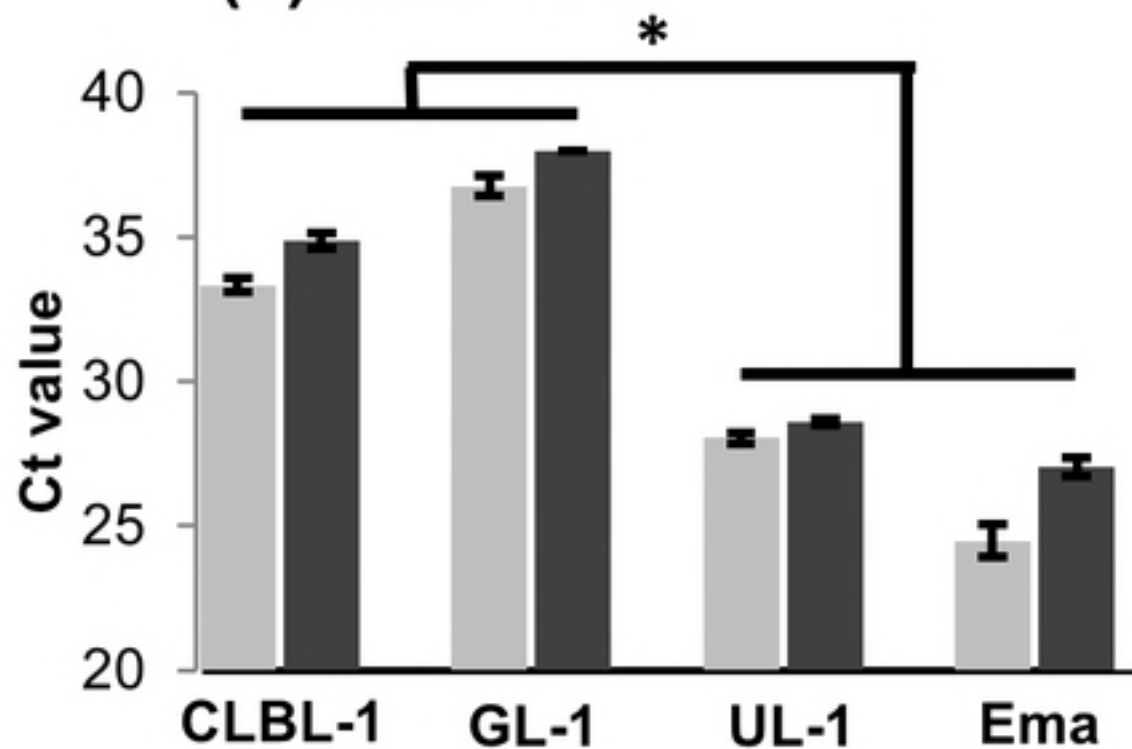
Figure



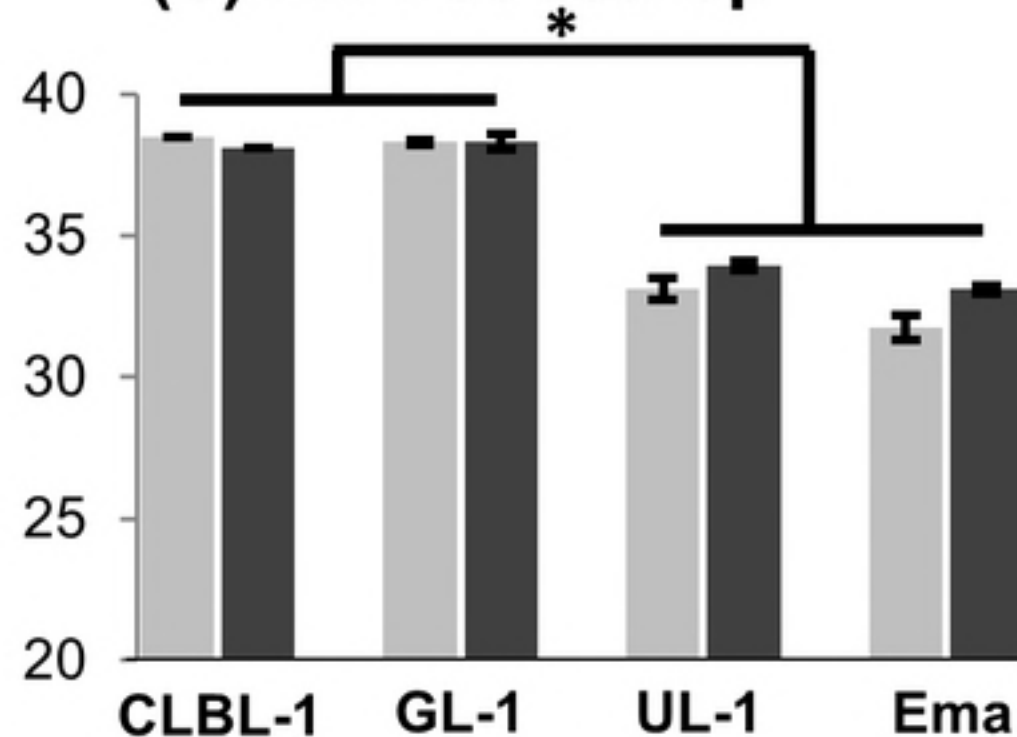


Figure

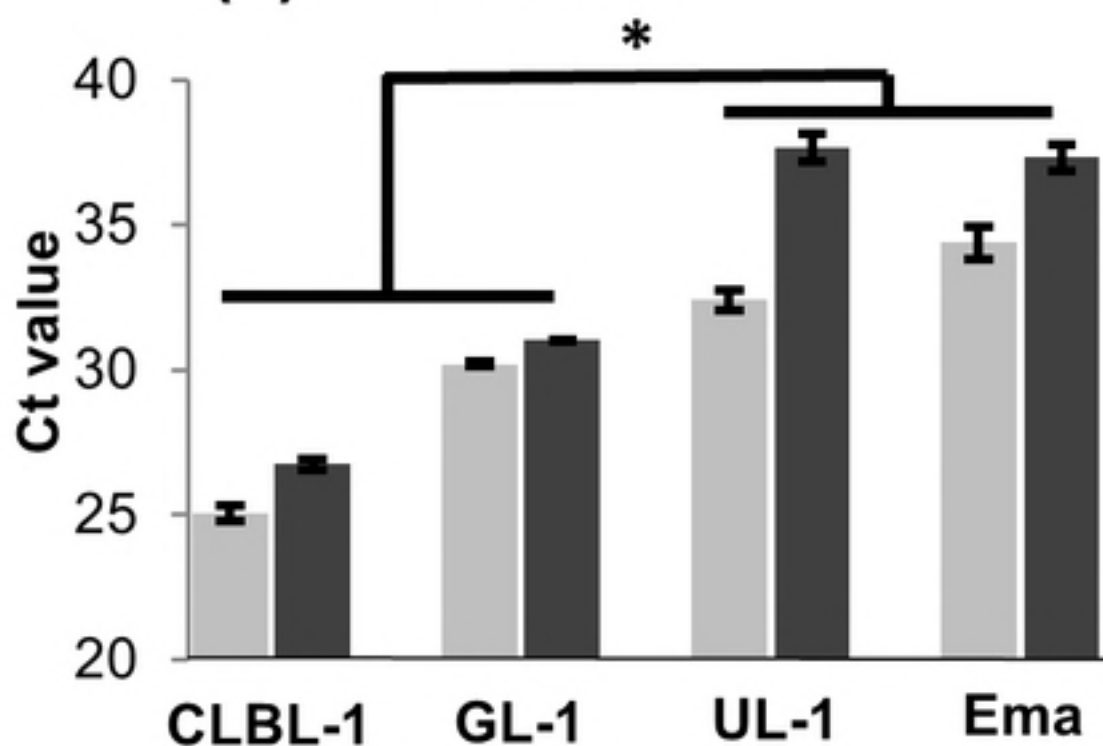
**(a) miR-151**



**(b) miR-8908a-3p**



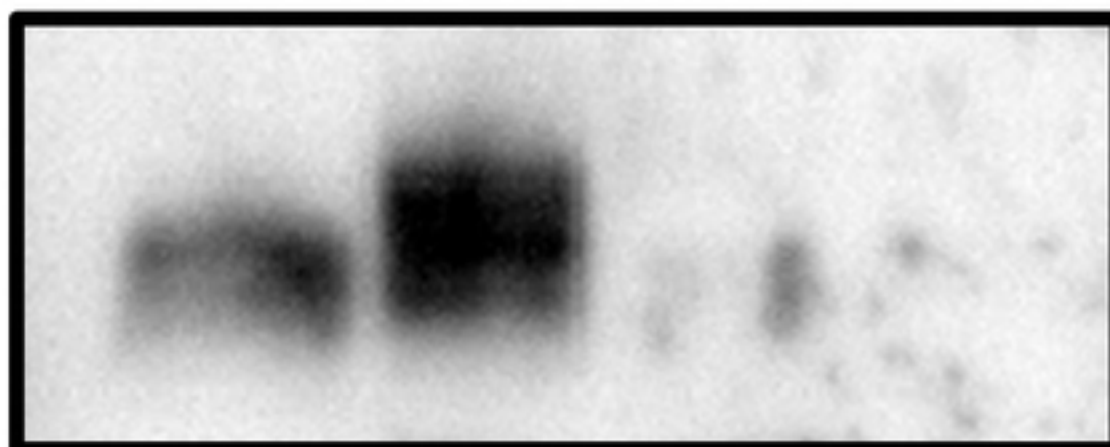
**(c) miR-486**



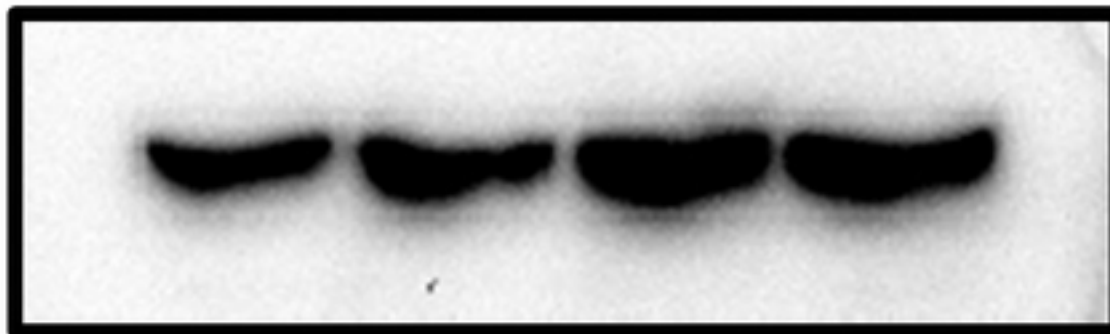
Exosome  
Cell

**(a) Exosome**

**CLBL-1 GL-1 UL-1 Ema**



**CD82**



**HSP90B**

**(b) Cell**

**CLBL-1**

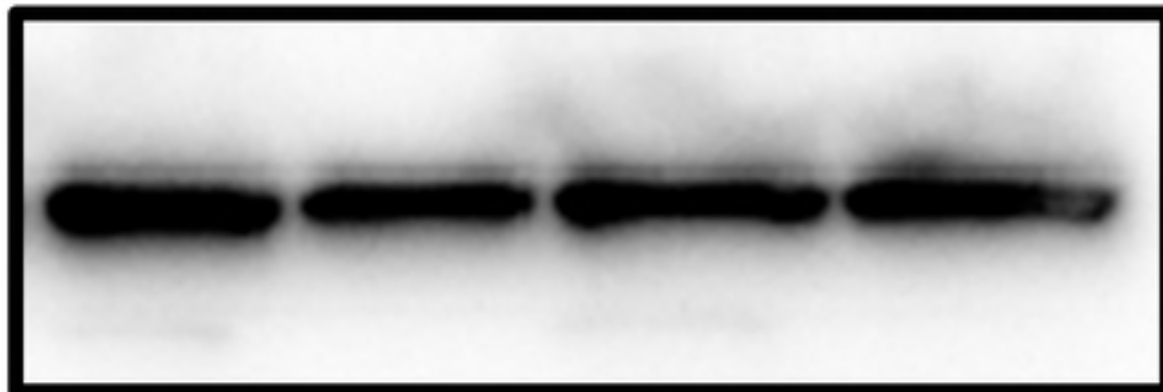
**GL-1**

**UL-1**

**Ema**



**CD82**



**$\beta$ -actin**